

Supporting information

First observation of $[\text{Pu}_6(\text{OH})_4\text{O}_4]^{12+}$ cluster during the hydrolytic formation of PuO_2 nanoparticles using H/D kinetic isotope effect

Manon Cot-Auriol ^a, Matthieu Virost ^a, Thomas Dumas ^b, Olivier Diat ^a, Denis Menut ^c
Philippe Moisy ^b, Sergey I. Nikitenko ^a

^a ICSM, Univ Montpellier, CEA, CNRS, ENSCM, Marcoule, France.

^b CEA, DES, ISEC, DMRC, Univ Montpellier, Marcoule, France.

^c Synchrotron SOLEIL, MARS beamline, l'Orme des Merisiers, Départementale 128, 91190 Saint Aubin, France.

I. Materials and methods

Synthesis of Pu(IV) intrinsic colloids

Experiments with plutonium were carried out at Atalante Facility, Marcoule (France). The concentrated Pu(IV) solution used was purified onto anion exchange resin and was stabilized in *ca.* 2.4 M HNO_3 . The isotopic composition (wt%) was 96.9% ^{239}Pu , 2.9% ^{240}Pu , 0.1% ^{242}Pu and 0.1% ^{238}Pu . Hydrolytic colloid suspensions were prepared by diluting a small volume of Pu(IV) concentrated solution with pure water (Milli-Q water, 18.2 $\text{M}\Omega\cdot\text{cm}$ at 25 °C) or pure deuterium oxide solution (D_2O), under vigorous stirring. The final concentration of Pu was 5 mM and the solutions showed a green emerald colour which is characteristic of the Pu(IV) colloid species. In some cases, the initial pH of H_2O or D_2O were adjusted by adding 0.1 M HNO_3 prepared in H_2O or D_2O , respectively.

Spectroscopic, SAXS and XAS characterizations

Plutonium solutions were analysed by Vis-NIR absorption spectroscopy with 1 cm cuvettes (UV3600 Shimadzu spectrophotometer, 350-900 nm range). SAXS and XAS characterizations were realized on the MARS beamline, at the SOLEIL Synchrotron Radiation Facility (Saint-Aubin, France; 2.75 GeV at 500 mA). The optical part was composed of a double-crystal monochromator (DCM) framed by two Pt-coated mirrors for beam collimation and rejection of higher-order harmonics. Energy calibration was made at the yttrium edge (17 038 eV). Plutonium samples were confined in a specific cell, which was composed of Teflon sample holders (slots of 250 μL) closed by Kapton[®] layers.

SAXS analyses were performed for 5 s acquisition time per sample, with an X-ray energy of 17 keV and a sample to detector (MAR345) distance of 764 mm. The beam stop was fixed in front of the detector and placed in a He gas reservoir in order to reduce the air scattering. The scattering intensity $I(Q)$ was obtained after averaging the isotropic 2D scattering data using Fit2D software. The final absolute scattering intensity for colloids was calculated by subtracting the empty cell, solvent and background contributions, and using a normalisation procedure with a benchmarked polyethylene sample. SAXS fitting procedure was performed using SASview 5.0 software.

XAS spectra were recorded in fluorescence mode at Pu L₃-edge (HPGe multi-element detector) with a sample orientation of 45° to the incident beam. A metallic Zr foil was used to calibrate the incident energy (K-edge defined at 17 988 eV). Pu ionization energy was defined at the maximum of the white line (E₀ = 18 068 eV) and each of the provided XAS spectrum results from an average of 3 scans acquired at the Pu L_{III} edge. In the case of D₂O, a XAS spectrum of Pu(VI) was subtracted from the experimental spectrum before fitting the data. EXAFS data analysis was carried out with Athena and Artemis software from the IFFEFIT package.^[1] Fits were performed with Artemis code (Kaiser-Bessel window, 2.7-13 Å⁻¹ k range). The fit of EXAFS data was based on the crystalline fcc PuO₂ structure with a two O-shell model (short oxygen and medium oxygen) for the first coordination sphere. The model was composed of four single scattering paths (O_s, O_m, Pu, O₂) with the distance Pu-O₂ (4.46 Å) and S₀² = 0.9 as fixed parameters. Pu and O₂ scattering paths describe the interactions in the second coordination sphere. Coordination numbers, Debye-Waller factors and others distances were considered as floating parameters.

Determination of the Pu(VI) concentration and the corresponding rate of Pu(VI) consumption

The Pu(VI) concentration (c) was calculated over time with the Beer-Lambert law (Eq. 1) by considering the absorbance value (A) at λ = 830 nm, with the molar absorption coefficient (ε) equal to 470 L·mol⁻¹·cm⁻¹ and the distance taken by the light in the sample (l) equal to 1 cm.^[2] The error was estimated at 10%.

$$A = \varepsilon \times l \times c \quad (\text{Eqn. S1})$$

Assuming that Pu(VI) consumption follows a first order reaction rate on Pu(VI), the following equation can be used.

$$\ln\left(\frac{[Pu^{VI}]_t}{[Pu^{VI}]_{max}}\right) = -kt \quad (\text{Eqn. S2})$$

Deconvolution of Vis-NIR absorption spectra

A deconvolution of the Vis-NIR spectra was performed to determine the participation of each species present in the solution. This treatment is based on the additivity of the absorbance (Eq. 3). A_i is the absorbance of the species i and a_i is the corresponding participation coefficient.

$$A_{total} = \sum_i a_i A_i \quad (\text{Eqn. S3})$$

Reference spectra for Pu(III), Pu(IV), Pu(VI) were used. Each one corresponds to a known concentration (Table S1). In the case of the colloid reference spectrum, it was obtained from a spectrum measured on an aged colloidal solution (> 1 month in H₂O), from which the participation of Pu(VI) was subtracted. We assumed that the rest of the Pu in solution was considered to be only in the colloid form. The same approach was applied to obtain a reference spectrum of the cluster, by subtracting the participation of Pu(III), Pu(IV), Pu(VI) and Pu colloid. The final reference concentration for the cluster was equaled to the difference between the Pu total concentration (5 mM) and the concentrations of the different subtracted

species. An illustration of the application of deconvolution is given in **Fig. S1**. The error is the difference between the experimental spectrum and the simulated spectrum (fit). To optimize the fit quality, the sum of the squares of the error (**Eq. 4**) must tend towards 0.

Table S1: Molar absorption coefficients (ϵ) and concentrations (c) of the plutonium references for Pu(III), Pu(IV), Pu(VI), Pu_{coll} and Pu_{cluster}. Pu(IV) is for hydrolyzed Pu(IV) species.

Species	λ (nm)	ϵ (L.mol ⁻¹ .cm ⁻¹)	C (mol.L ⁻¹)
Pu(III)	601	39	0.002
Pu(IV)	475	70	0.011
Pu(VI)	830	470	0.003
Pu _{coll}	616	17	0.005
Pu _{cluster}	-	-	0.003

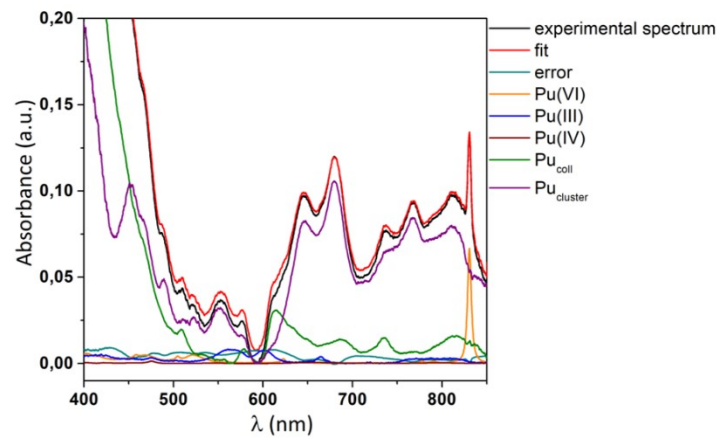


Fig. S1: Deconvolution result of the Vis-NIR absorption spectrum obtained at 2 min after dilution of the concentrated Pu(IV) solution in H₂O.

$$Error_{total} = \sum_{\lambda} (A_{exp}(\lambda) - A_{fit}(\lambda))^2 \quad (\text{Eqn. S4})$$

Determination of the colloid formation rate

The determination of the colloid formation rate is based on the deconvolution of experimental Vis-NIR spectra. After extracting the contribution of the colloid spectral signature in the experimental spectra, the colloid concentration in the solution can be plotted as a function of time. Assuming that the colloid formation reaction is total and with a first order, the rate can be calculated by using the following equation.

$$\ln\left(1 - \frac{[Pu_{coll}]_t}{[Pu_{coll}]_{max}}\right) = -kt \quad (\text{Eqn. S5})$$

Theoretical isotopic separation factor for OH/OD bonds splitting

The isotopic separation factor ($\alpha_{(H/D)}$) is calculated using semiclassical zero-point energy approximation according to the **Eq. 6**. ΔE is the zero-point energy difference for OH/OD bonds ($\Delta E = 5.89$ kJ.mol⁻¹), R is the molar gas constant and T is the temperature.

$$\alpha_{(H/D)} = e^{\left(\frac{\Delta E}{RT}\right)} \quad (\text{Eqn. S6})$$

SAXS fitting model

The definition of the SAXS scattering diagrams for diluted systems is generally based on the Eq. 7, with ϕ the volume fraction, $P(Q)$ the form factor related to size and shape of the scattering objects and $S(Q)$ the structure factor related with particle interactions. Due to the low concentration of colloidal particles, we considered the absence of interaction between them, which means that the last parameter $S(Q)$ is equal to 1.

$$I(Q) = \Phi P(Q)S(Q) \quad (\text{Eqn. S7})$$

For the data adjustment, an approach was applied for the form factor $P(Q)$ using a model for homogeneous spheres with a Gaussian size distribution. For this model, there are four parameters with ϕ the volume fraction, R the particle radius, $\Delta\rho$ the scattering length density difference and PD the polydispersity (ratio between the half width of the Gaussian distribution function and the particle radius). The theoretical volume fraction was estimated at $\phi_{\text{th}} = 1.2 \cdot 10^{-4}$, considering a full conversion of plutonium solution into PuO_2 particles. Theoretical $\Delta\rho$ could be calculated from molar volume and considering dense oxide PuO_2 particles. All parameters used for fit application are summarized in **Table S2** and **S3**.

Table S2: Molar volume (V_m), X-ray scattering length density (ρ) and the corresponding difference $\Delta\rho$ used for SAXS diagram simulation calculations. Values for PuO_2 are based on the dense oxide density ($d = 11.5$).

	V_m (10^{-23} cm^3)	ρ (10^{10} cm^{-2})		$\Delta\rho$ (10^{10} cm^{-2})
PuO_2	3.99	77.78		
H_2O	2.99	9.42	$\text{PuO}_2/\text{H}_2\text{O}$	68.36
D_2O	3.00	9.41	$\text{PuO}_2/\text{D}_2\text{O}$	68.37

Table S3: SAXS data fitting parameters for a homogeneous sphere model with a Gaussian distribution in radius around a mean value R and a polydispersity value (PD). ϕ and $\Delta\rho$ being respectively the volume fraction and the scattering length density difference between the particle and the aqueous solvent.

Solvent	Sphere model			
	R (nm)	PD	ϕ_p (10^{-4})	$\Delta\rho$ (10^{10} cm^{-2})
H_2O	0.9 ± 0.1	0.15	1.5	69.2
D_2O	1.1 ± 0.1	0.15	0.75	69.0

II. pH effect

Light and heavy waters did not have the same initial pH_i value (**Table S4**). To check that this parameter did not affect the kinetics observed by Vis-NIR absorption spectroscopy, their pH_i was adjusted by adding 0.1 M HNO_3 (prepared in the corresponding medium) before adding the concentrated Pu(IV) solution (**Table S4**). The corresponding Vis-NIR spectra obtained in such conditions (not shown) did not exhibit any real differences from those presented in **Fig. S3**. This observation could be confirmed by SAXS analyses, where no differences were noted in the SAXS diagrams (**Fig. S2**). So, it can be assumed that the initial pH of the solvents (H_2O , D_2O) has no influence on the kinetics of Pu(IV) colloid formation. This may be explained by the high acidity of the concentrated Pu(IV) solution which will control the final pH of the Pu colloidal solution.

Table S4: measured pH values before adding Pu(IV) concentrated solution in H₂O and D₂O, and after synthesis of 5 mM Pu(IV) hydrolytic colloids (approx. 1 month old). *solvent pH modified by adding HNO₃ 0.1 M prepared in H₂O and D₂O, respectively. All values have an error of ± 0.2.

	H ₂ O		D ₂ O	
pH _i before synthesis	5.5	5.3*	5.9	5.4*
pH _f after synthesis	2.2	1.1	1.6	1.2

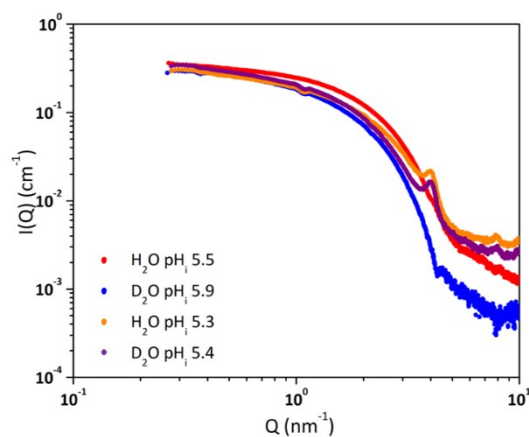


Fig. S2: SAXS diagrams of 5 mM Pu(IV) hydrolytic colloids formed in H₂O (red and orange dots) and D₂O (blue and purple dots), with two different starting pH_i for each solvent. The samples were 1 month old. The oscillation at Q = 4 nm⁻¹ is an artefact attributed to the scattering of the Kapton windows of the sample holder.

III. ESI figures and tables

Figure S3

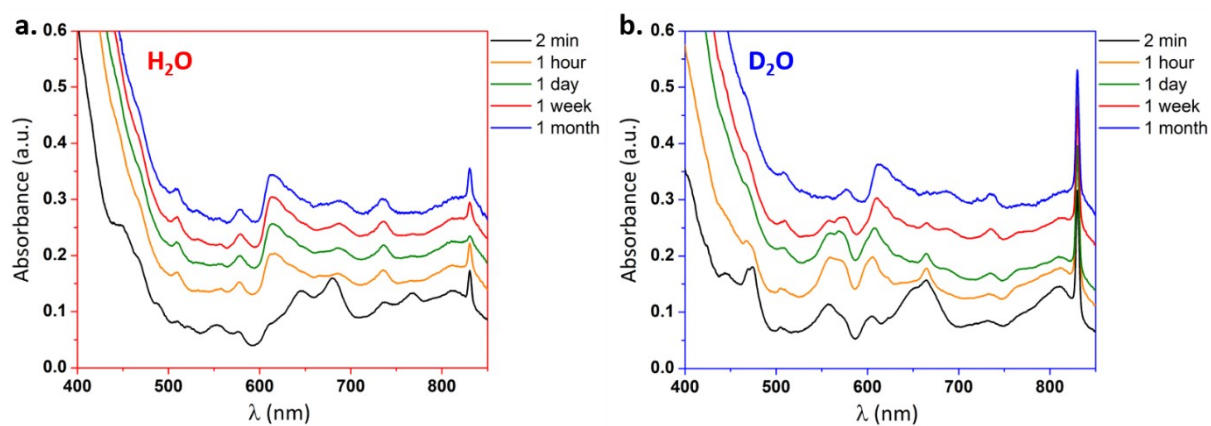


Fig. S3: Vis-NIR absorption spectra acquired over time during the synthesis of 5 mM Pu(IV) hydrolytic colloids in (a) H₂O and (b) D₂O.

Figure S4

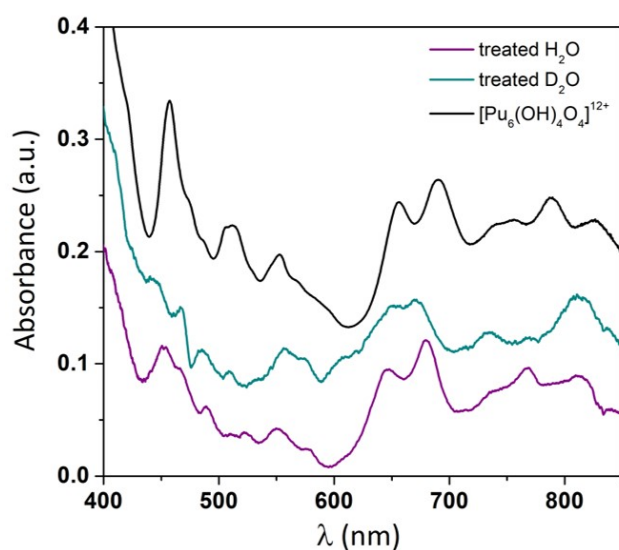


Fig. S4: Vis-NIR absorption spectra just after the dispersion of Pu(IV) concentrated solution in H₂O (purple line) and D₂O (blue line). Spectra were previously treated by subtracting the Pu(IV), Pu(III), Pu(VI) and Pu colloid contributions. The Vis-NIR absorption spectrum of Pu(IV) acetate hexanuclear cluster (black line) was carried out for comparison, with courtesy of C. Tamain.^[3]

Figure S5

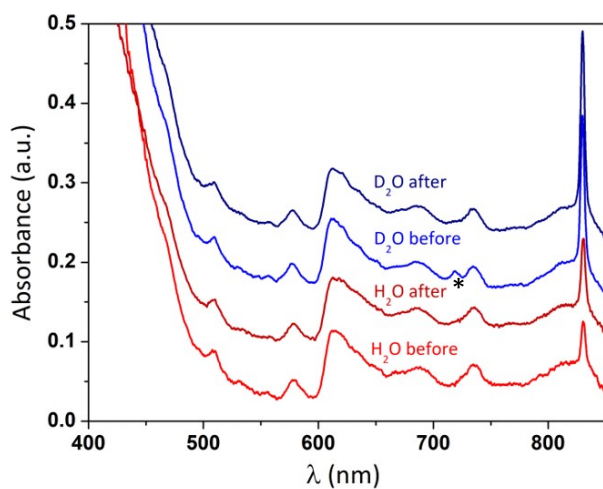


Fig. S5: Vis-NIR absorption spectra before and after synchrotron analyses acquired on 5 mM Pu(IV) hydrolytic colloids in (a) H₂O and (b) D₂O. (* artefact due to optic fibers)

Figure S6

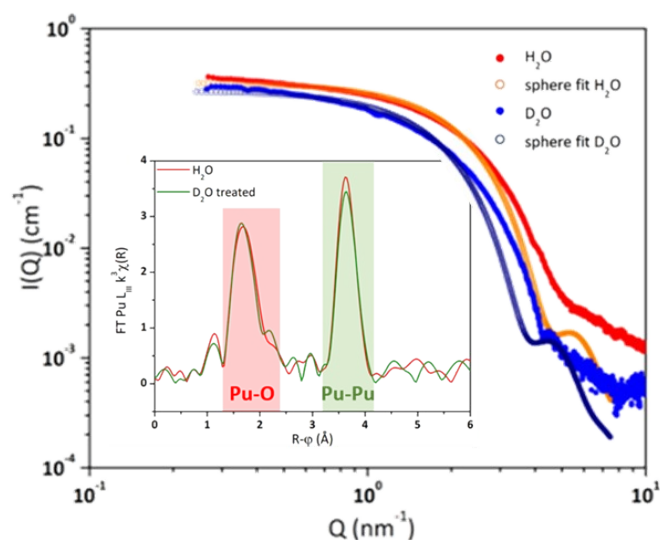


Fig. S6: SAXS diagrams of Pu(IV) colloids formed in H_2O and D_2O and corresponding fits. Inset: k^3 -weighted FT for Pu(IV) colloids (H_2O and D_2O , without Pu(VI) contribution).

Figure S7

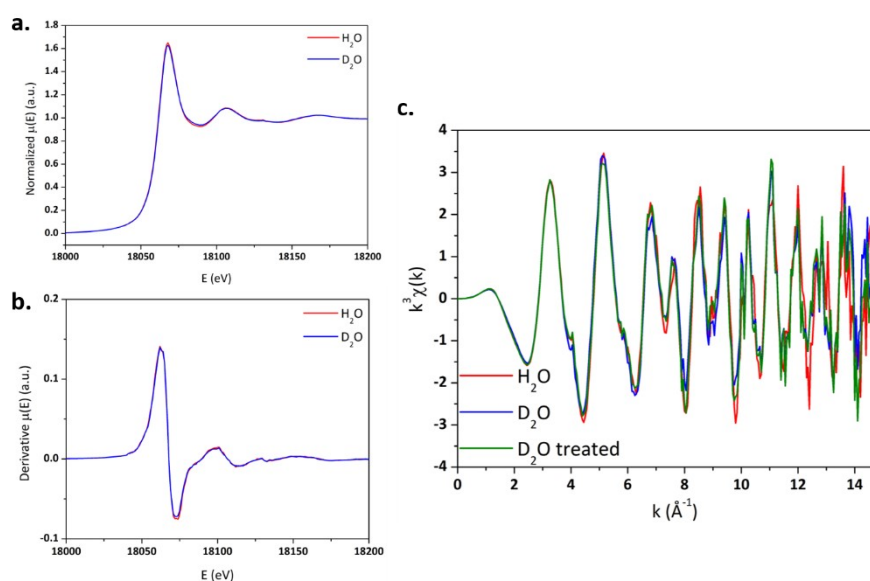


Fig. S7: (a) Pu-L₃ XANES and (b) corresponding derivative for 5 mM Pu(IV) hydrolytic colloids (1 month old) formed in H_2O (red line) and D_2O (blue line). (c) k^3 -weighted experimental EXAFS spectra acquired on 5 mM Pu(IV) hydrolytic colloids (1 month old) formed in H_2O (red line) and D_2O (blue line).

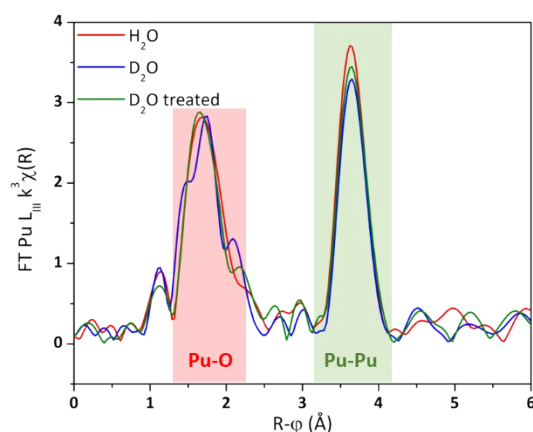
Figure S8

Fig. S8: Fourier transforms (FT) of the k^3 -weighted 2.709-13 \AA^{-1} range for Pu(IV) colloids formed in H_2O and D_2O . The green FT corresponds to the one of D_2O sample without Pu(VI) contribution.

Table S5

Table S5: EXAFS structural parameters of 5 mM Pu(IV) hydrolytic colloids formed in H_2O and D_2O , from k^3 -weighted EXAFS spectra (CN: coordination number, R: interatomic distance, σ^2 : Debye-Waller factor). (*) $R_{\text{Pu-O}_2} = 4.46 \text{ \AA}$ was fixed according to the crystalline fcc PuO_2 structure. $S_0^2 = 0.9$, $\Delta E_0 = 2.97$ -3.74 eV. R-factor < 5%. The standard deviations measured using IFFEFIT software are given in parentheses.

PuO ₂	H ₂ O			D ₂ O after Pu(VI) subtraction		
	CN	R (Å)	σ^2 (Å ²)	CN	R (Å)	σ^2 (Å ²)
Pu-O _s	5.4(62)	2.26(8)	0.008(6)	6.3(26)	2.27(3)	0.009(4)
Pu-O _m	3.4(64)	2.42(11)	0.008(10)	2.3(24)	2.44(4)	0.004(4)
Pu-Pu	5.6(9)	3.80(1)	0.006(1)	5.6(10)	3.81(1)	0.007(1)
Pu-O ₂	11.2(18)	4.46*	-	11.1(20)	4.46*	-

References

- [1] B. Ravel, M. Newville, *J. Synchrotron Rad.* **2005**, *12*, 537–541.
- [2] D. Jebaraj Mahildoss, T. N. Ravi, *J Radioanal Nucl Chem* **2012**, *294*, 87–91.
- [3] G. Chupin, C. Tamain, T. Dumas, P. L. Solari, P. Moisy, D. Guillaumont, *Inorg. Chem.* **2022**, *61*, 4806–4817.